THE AMERICAN SOCIETY OF MECHANICAL ENGINEERS
345 E. 47th St., New York, N.Y. 10017

95-GT-191

BLADE PITCH INFLUENCE AT THE EXIT FLOW FIELD OF AN AXIAL FLOW FAN

Rafael Ballesteros
Eduardo Blanco
Carlos Santolaria
Departamento de Energía
Universidad de Oviedo
Gijón, Spain

ABSTRACT

Variable pitch axial flow fans are widely used in industrial applications to satisfy variable operating conditions. In this work, an experimental research on a fan of this kind has been carried out. The performance curves of the fan have been obtained and the flow field has been measured at the best efficiency point of each blade pitch tested and for a lower and higher flow rate, in a fixed plane downstream the rotor with a triple hot-wire probe. The radial and circumferential distributions have been obtained, and maps of the velocity components over a blade channel are shown for each operating condition. The flow structure, including the tip and hub blockage, the blade wakes and the main flow core, is characterized.

NOMENCLATURE

C : absolute velocity
Cm : average axial velocity Q/S
P : total pressure
Q : flow rate
R : radius ratio r / r_t
S : annulus area $\pi (r_t^2 - r_h^2)$
U : blade velocity
ρ : air density
ϕ : flow coefficient Cm / U_t
ψ : pressure coefficient $(P_2 - P_1) / (0.5 \rho U_t^2)$

Subscripts
ax : axial
h : at the hub
t : at the tip
tg : tangential
1 : inlet
2 : exit

1 INTRODUCTION

Many industrial ventilation systems require a wide operating range. One of the more efficient methods to fulfill the regulation purpose in axial flow fans is to provide variable pitch blades (Marples, 1982; O'Neill, 1982). However, changes in the performance curves occur in such a way that the stall margin is modified and the maximum efficiency is reduced. The pitch change implies that the blade geometry is not as well adapted to the resulting flow as in the design setting. This is due to the fact that the attack angle changes the same amount for each blade section, which have different sensitivity to that change.

In this work, an experimental research has been carried out on an axial flow fan with variable pitch. First of all, the fan performance curves have been obtained. Then, the flow field has been measured both at the inlet and the exit rotor plane using a triple hot-wire probe. The objective is to characterize the blade pitch influence and the operating conditions on the flow structure. Thus, maps of the velocity components over a blade

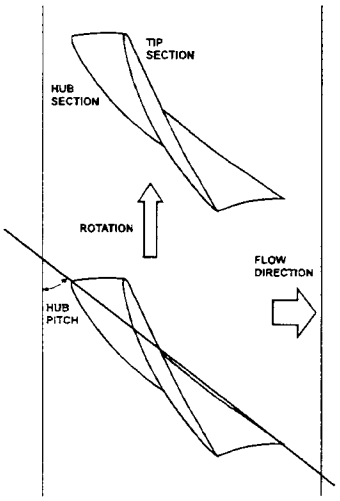

Figure 1. Angular reference

Presented at the International Gas Turbine and Aeroengine Congress and Exposition
Houston, Texas - June 5-8, 1995

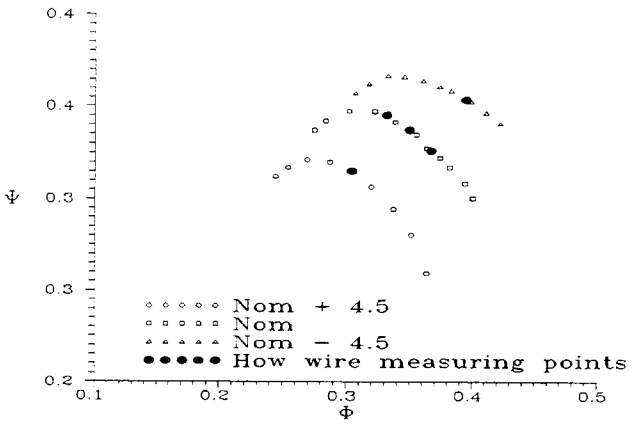

Figure 3. Pressure coefficient against flow coefficient

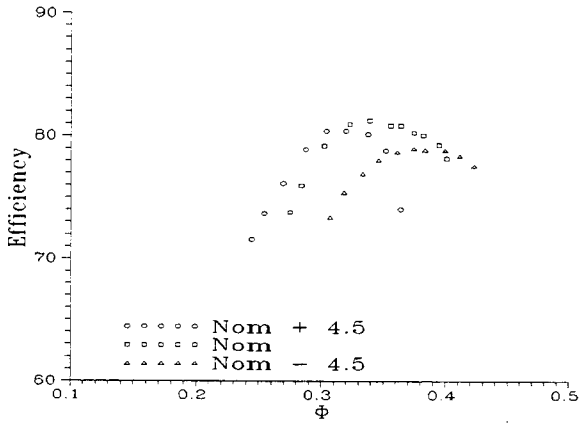

Figure 4. Efficiency versus flow coefficient

each blade pitch tested, and for a lower and higher flow rate. The measurement exit and inlet planes are 142 mm downstream and 120 mm upstream the blade axis, respectively. In both planes, ten radial positions were selected (Figure 5). In each one the signals coming from the three wires were acquired, together with one pulse per revolution trigger signal. This signal was used to accurately position the different radial signals among themselves.

The data were acquired with an analog-to-digital card placed in a personal computer, stored in files and transformed according with the calibration charts of the probe to obtain both the flow velocity and the flow angle. Data acquisition frequency was 12.8 kHz per channel (256 points per revolution) to obtain a good resolution and the filtering frequency was set to 5 kHz per channel to avoid acquisition errors (aliasing). Meaning frequencies in the flow are lower than 1 kHz. The acquisition length was 2304 points per channel.

For each flow condition tested, the averaging of the acquired signals made possible to obtain either the radial and the circumferential distribution of each velocity component.

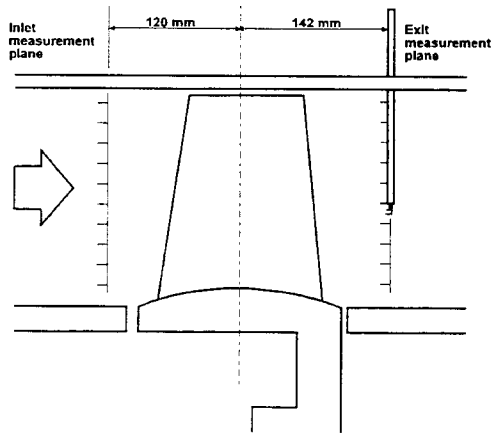

Figure 5. Flow measurement positions

3 RESULTS

In the following figures, the velocity components will appear in a dimensionless way: the axial component with respect to the mean axial velocity in each particular test condition, and the radial and tangential components with respect to the tip blade velocity, U_t.

Mean radial distributions

These distribution have been obtained by averaging all the circumferential data to one value for each radial position. At the inlet plane, the flow is almost axial and quite uniform from hub to tip. Figure 6 shows the radial distribution of the axial component at both the inlet and exit rotor measurement planes for the design geometry and the best efficiency point.

With respect to the exit plane, the axial component is uniform except in the tip region. The blockage due to the end-wall boundary layer present at the inlet plane has increased considerably through the rotor.

Figure 7 shows the radial distribution of the tangential components for the same conditions. It decreases from hub to mid-span, presenting a free vortex distribution modified by the blockage in the tip region.

Velocity maps

The maps have been obtained by averaging each radial measurement to the circumferential extent of two blade channels and by relatively positioning them in such a way that the circumferential origin be the same. Thus, the flow field can be seen from hub to tip and from blade to blade. For a fixed blade setting, due to the pitch and chord change from hub to tip, the distance from the measurement exit plane to the trailing edge varies from hub to tip. This distance is also different for each blade setting. This fact implies that the blade wakes diffusion rates will not be constant.

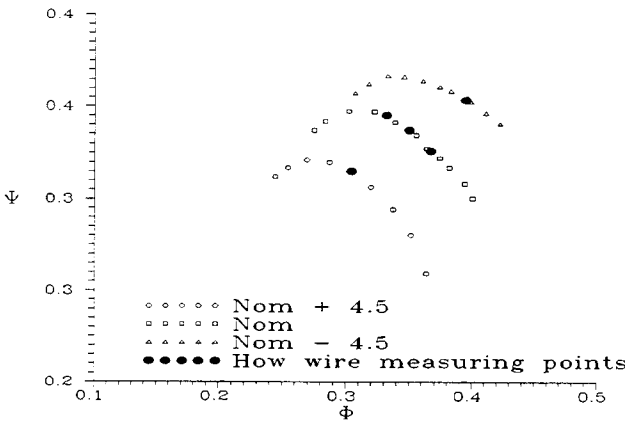

Figure 3. Pressure coefficient against flow coefficient

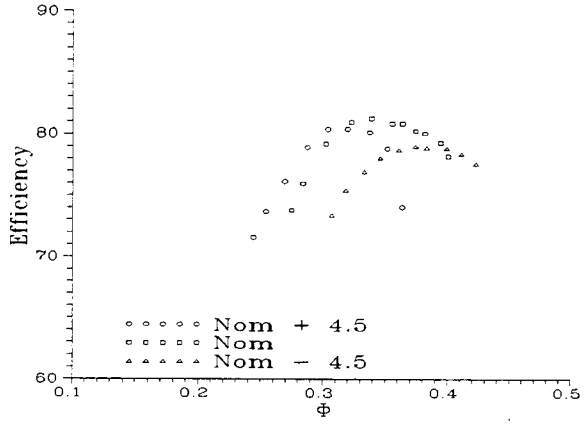

Figure 4. Efficiency versus flow coefficient

each blade pitch tested, and for a lower and higher flow rate. The measurement exit and inlet planes are 142 mm downstream and 120 mm upstream the blade axis, respectively. In both planes, ten radial positions were selected (Figure 5). In each one the signals coming from the three wires were acquired, together with one pulse per revolution trigger signal. This signal was used to accurately position the different radial signals among themselves.

The data were acquired with an analog-to-digital card placed in a personal computer, stored in files and transformed according with the calibration charts of the probe to obtain both the flow velocity and the flow angle. Data acquisition frequency was 12.8 kHz per channel (256 points per revolution) to obtain a good resolution and the filtering frequency was set to 5 kHz per channel to avoid acquisition errors (aliasing). Meaning frequencies in the flow are lower than 1 kHz. The acquisition length was 2304 points per channel.

For each flow condition tested, the averaging of the acquired signals made possible to obtain either the radial and the circumferential distribution of each velocity component.

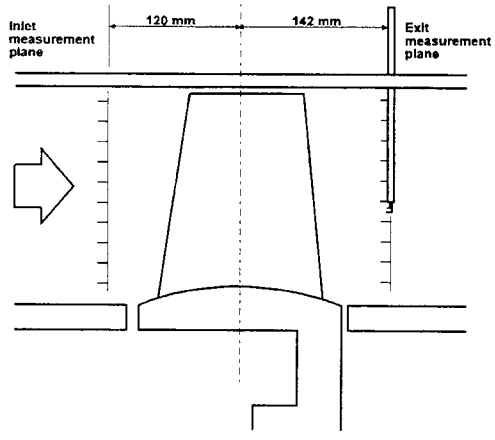

Figure 5. Flow measurement positions

3 RESULTS

In the following figures, the velocity components will appear in a dimensionless way: the axial component with respect to the mean axial velocity in each particular test condition, and the radial and tangential components with respect to the tip blade velocity, U_t.

Mean radial distributions

These distribution have been obtained by averaging all the circumferential data to one value for each radial position. At the inlet plane, the flow is almost axial and quite uniform from hub to tip. Figure 6 shows the radial distribution of the axial component at both the inlet and exit rotor measurement planes for the design geometry and the best efficiency point.

With respect to the exit plane, the axial component is uniform except in the tip region. The blockage due to the end-wall boundary layer present at the inlet plane has increased considerably through the rotor.

Figure 7 shows the radial distribution of the tangential components for the same conditions. It decreases from hub to mid-span, presenting a free vortex distribution modified by the blockage in the tip region.

Velocity maps

The maps have been obtained by averaging each radial measurement to the circumferential extent of two blade channels and by relatively positioning them in such a way that the circumferential origin be the same. Thus, the flow field can be seen from hub to tip and from blade to blade. For a fixed blade setting, due to the pitch and chord change from hub to tip, the distance from the measurement exit plane to the trailing edge varies from hub to tip. This distance is also different for each blade setting. This fact implies that the blade wakes diffusion rates will not be constant.

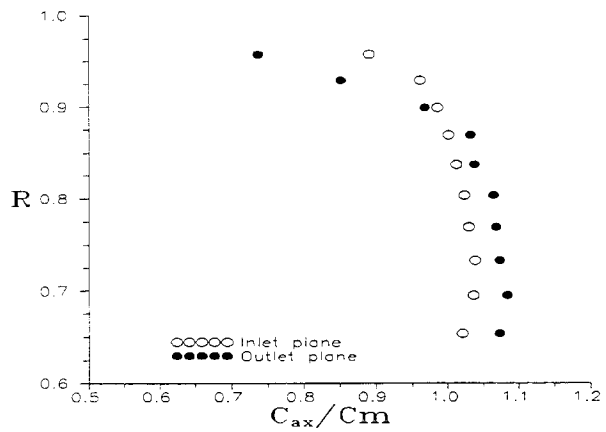

Figure 6. Radial distribution of the dimensionless axial component

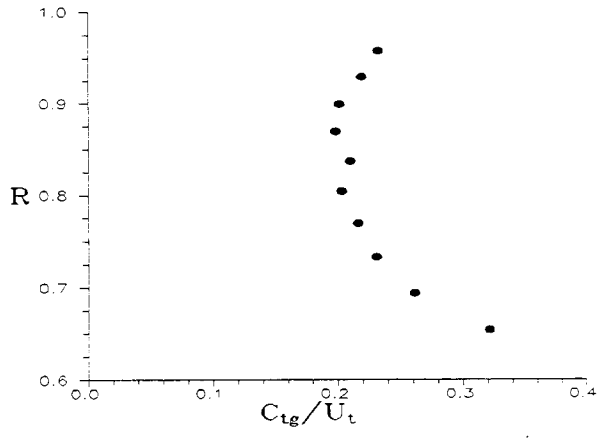

Figure 7. Radial distribution of the dimensionless tangential component

The incoming flow to the rotor scarcely changes from blade to blade. Thus, only maps at the exit plane are presented. The maps represent an instant picture of the flow field seen from downstream the rotor, which would be turning anti-clockwise. In a blade wake, the right side comes from the blade suction side.

Next, either the flow rate influence and the blade pitch influence on the flow structure is to be analyzed. Figure 8 shows the map of the radial component for the design conditions. This component is small except in the blade wakes where it increases slightly. Similar trends were found for the other test conditions.

- Flow rate influence

Figure 9 shows the maps corresponding to the axial component for the three flow rates in the design geometry. In each map can be seen a core of high axial component corresponding with the area between the blade wakes and the boundary layer blockage both in the hub and the tip region. The blockage due to the boundary layer in the tip region is bigger than in the hub region. It can be observed that if the flow rate decreases the wake gets wider, mainly in the tip region: the same increment of the incidence angle implies a relative bigger increase of the deflexion at the tip. Also, the wake leans clockwise because as the distance between the trailing edge and the measurement plane is longer at the tip than at the hub, when the axial velocity decreases, the lapse between the arrival of the hub flow and the tip flow to the measurement plane increases.

The maps corresponding to the tangential component for the three flow rates in the design geometry are presented in figure 10. As already mentioned when describing the radial distributions in the exit plane, the higher values are concentrated in the hub region due to the wider blade wakes, the hub boundary layer and the higher loading imposed. When the flow rate decreases, the value of this component increases both in the wakes and in the core. The increase of work, at least in the flow rate range tested, is achieved by increasing the extent of the higher values zone more than by increasing the maximum values. Also, the core seems to shift towards the tip pressure side.

- Blade pitch influence

Figure 11 shows the maps corresponding to the axial component for the optimum flow rates (maximum efficiency point) in the three pitches tested. In this case, the blockage and the blade wakes at the tip increase as the blade pitch decreases; also, the core shifts towards the hub suction side. This can be explained because of the higher relative reduction of the blade channel at the tip with the pitch decrement. Besides, -what can be seen even with an inviscid simulation (Ballesteros, 1992)- the decrease of the pitch implies a movement backwards of the maximum velocity on the suction side and thus a higher gradient and the subsequent increase of the boundary layer thickness. As previously mentioned, decreasing the pitch the wake leans clockwise not only due to the lower flow rate of the different optimum points but also because of the longer distances between the trailing edge and the measurement plane.

The corresponding tangential components are shown in figure 12. Again, the higher values are concentrated in the hub region for the same reasons than before. When the blade pitch decreases, the value of this component decreases everywhere. The shift of the axial component core towards the hub, where the higher tangential components are present, causes the difference between the maximum and the minimum value to be reduced. This reduction of gradients is also affected by the longer distance between the trailing edge to the measurement plane when decreasing the pitch; as stated by Lakshminarayana et al., 1982, the decay rate of the tangential component defect is faster with distance than the corresponding one of the axial component.

4 CONCLUSIONS

An experimental research on an axial flow fan with variable pitch has been carried out. The performance curves of the fan have been obtained and the flow field has been measured at the best efficiency point of each blade pitch tested and for a lower and higher flow rate, in a fixed plane downstream the rotor with a triple hot-wire probe. The radial and circumferential distributions have been obtained, and maps of the velocity components over a blade channel are shown for each operating condition.

The tip blockage increases substantially from the inlet to the exit rotor plane, especially with the blade pitch decrement. Thus, the tangential component presents the free vortex design distribution modified by this blockage.

At the tip, the wake width increases and leans backwards when the flow rate or the pitch decreases.

The axial component core shifts towards the hub suction side because of the higher relative reduction of the blade channel at the tip with the pitch decrement. This shift towards the higher tangential components zone smooths the difference between the maximum and the minimum value of the tangential component.

For a fixed blade setting the differences of work with the flow rate are achieved by the extent change of the higher values zone of the tangential component more than by the change of the maximum values.

REFERENCES

Ballesteros, R., "Modelización del Flujo en Ventiladores Axiales de Paso Variable" (in spanish), Ph.D. Thesis, Un. of Oviedo, Spain, 1992.

Blanco, E., "Desprendimiento Rotativo en Ventiladores Axiales de Paso Variable" (in spanish), Ph.D. Thesis, Un. of Oviedo, Spain, 1992.

Breugelmans, F.A.E., Blanco, E., "Three Dimensional Flow Measurements in the Relative Frame of Reference during Rotating Stall", *Proceedings of the X International Symposium on Air Breathing of Engines*, AIAA, Nottingham, England, 1991.

British Standard BS-848, "Fans for General Purposes. Part I. Methods of Testing Performance", 1980.

Lakshminarayana, B., Govindan, T.R., Reynolds, B., "Effects of Rotation and Blade Incidence on Properties of Turbomachinery Rotor Wake", *AIAA Journal*, Vol. 20, Feb. 1982, pp. 245-253.

Marples, J., "A Discussion of Fan Air Quantity Control with Particular Respect to Axial Flow Fans and Variable Pitch Mechanisms", *Proceedings of the BHRA International Conference on Fan Design & Applications*, paper K2, pp. 445-459, Guilford, England, 1982.

O'Neill, A.C., "Variable Pitch Axial Flow Fans", *Proceedings of the BHRA International Conference on Fan Design & Applications*, paper K3, pp. 461-499, Guilford, England, 1982.

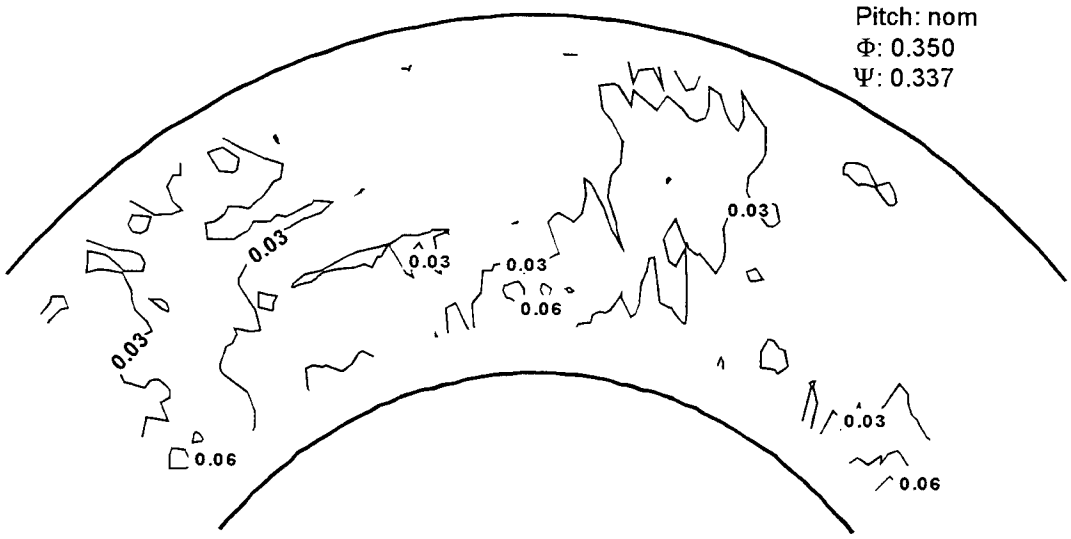

Figure 8. Radial component map at the exit plane

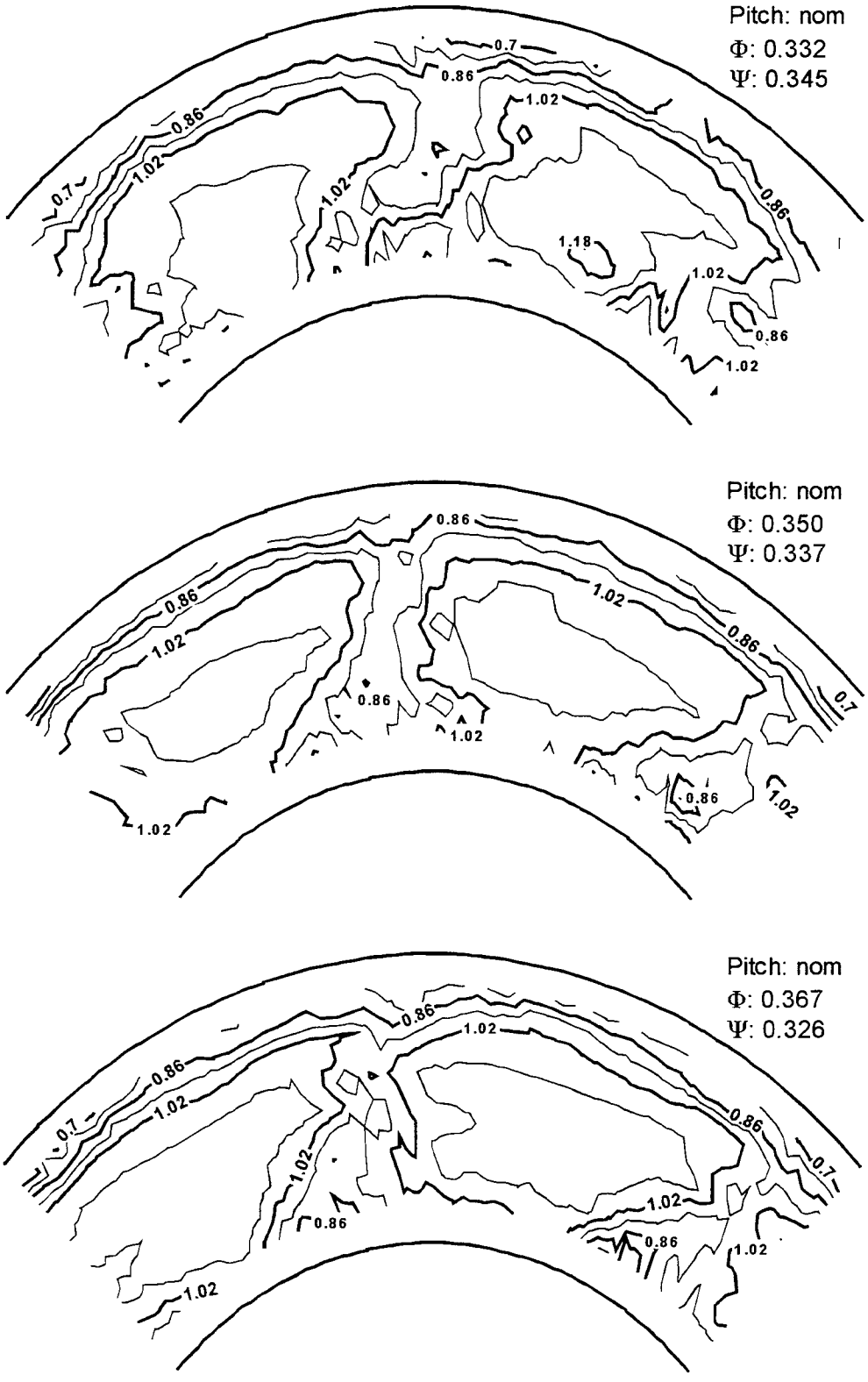

Figure 9. Axial component map at design geometry
for the three flow rates tested

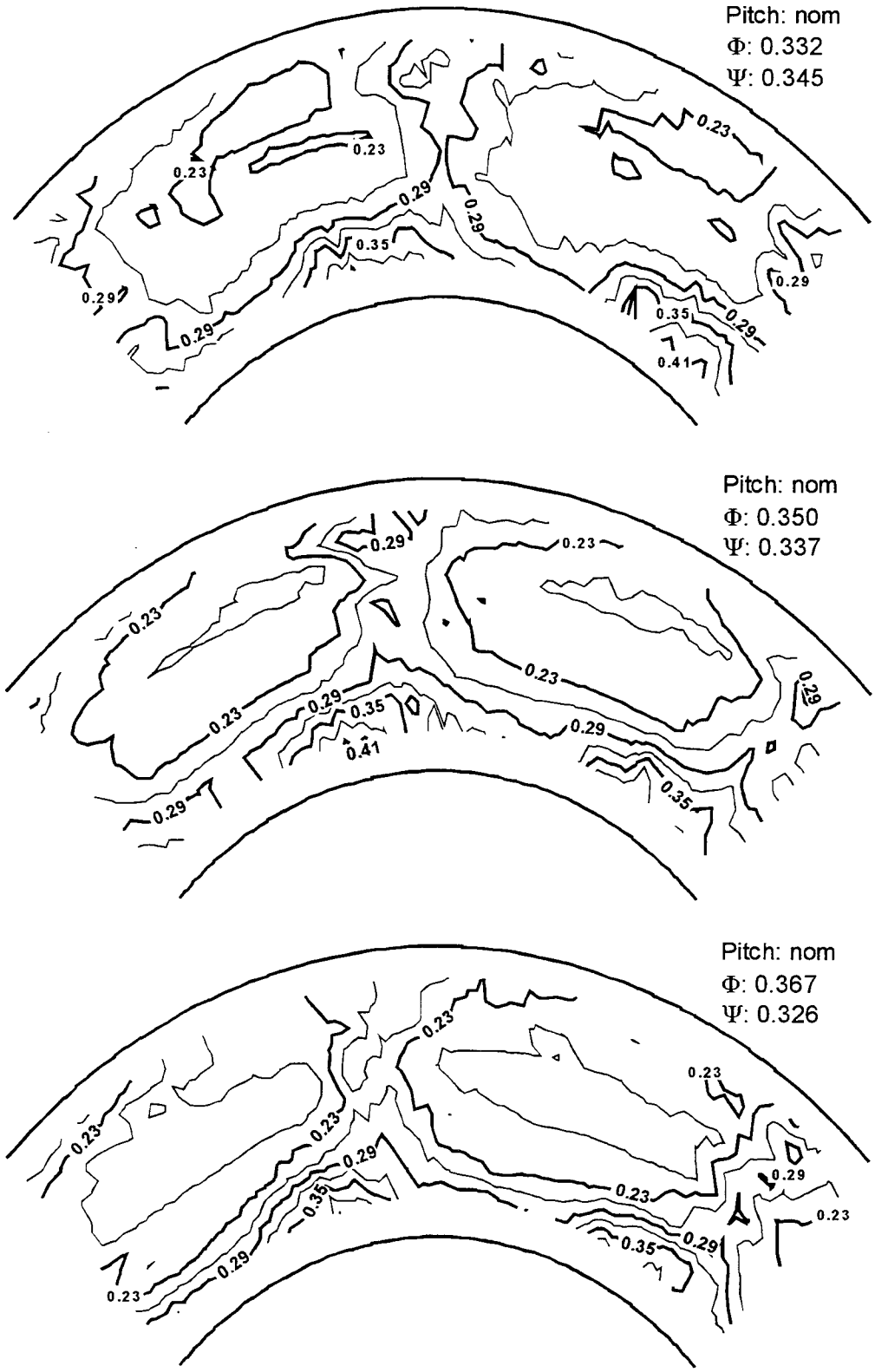

Figure 10. Tangential component map at design geometry for the three flow rates tested

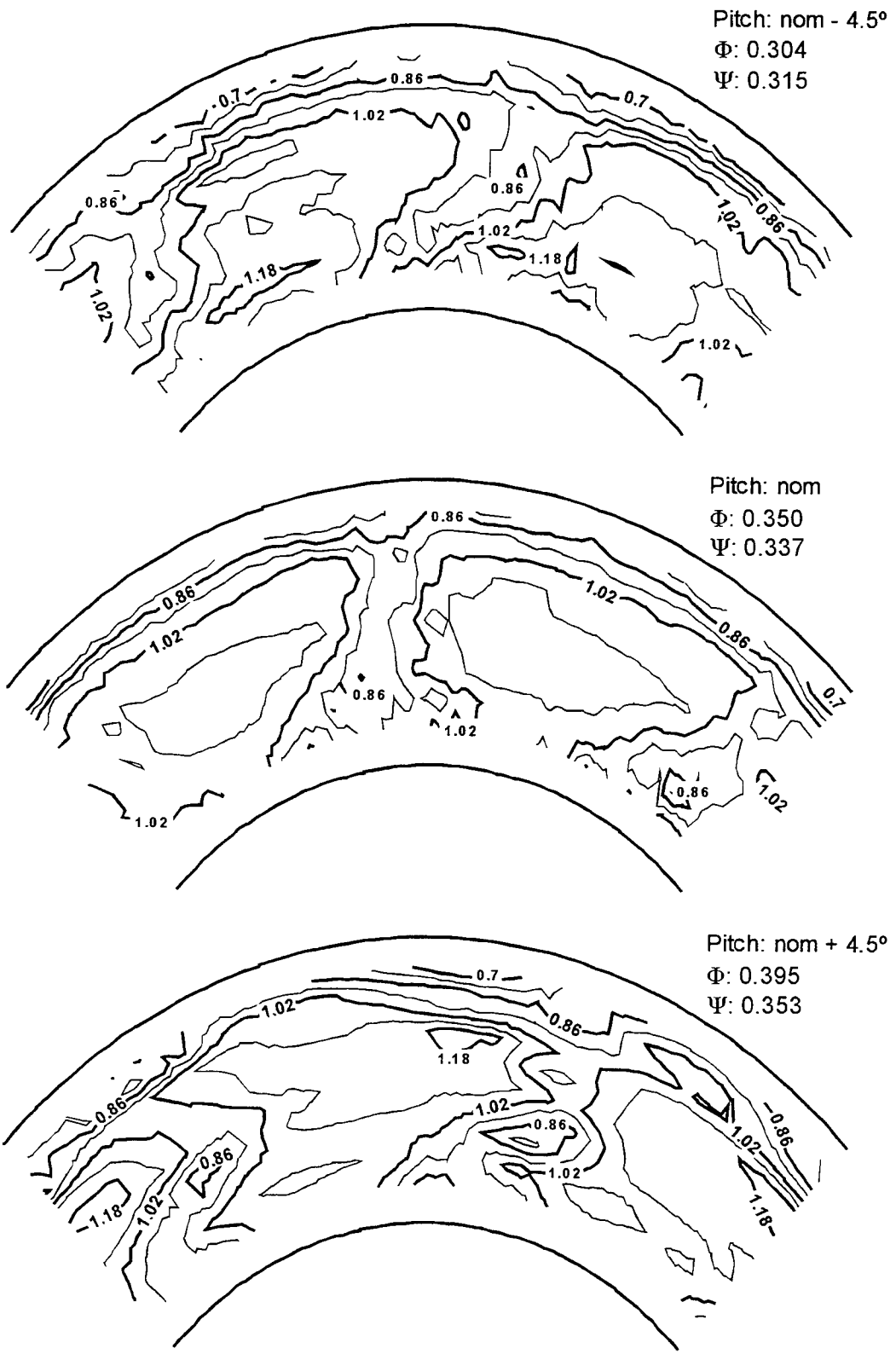

Figure 11. Axial component map at optimum flow rate for the three pitches tested

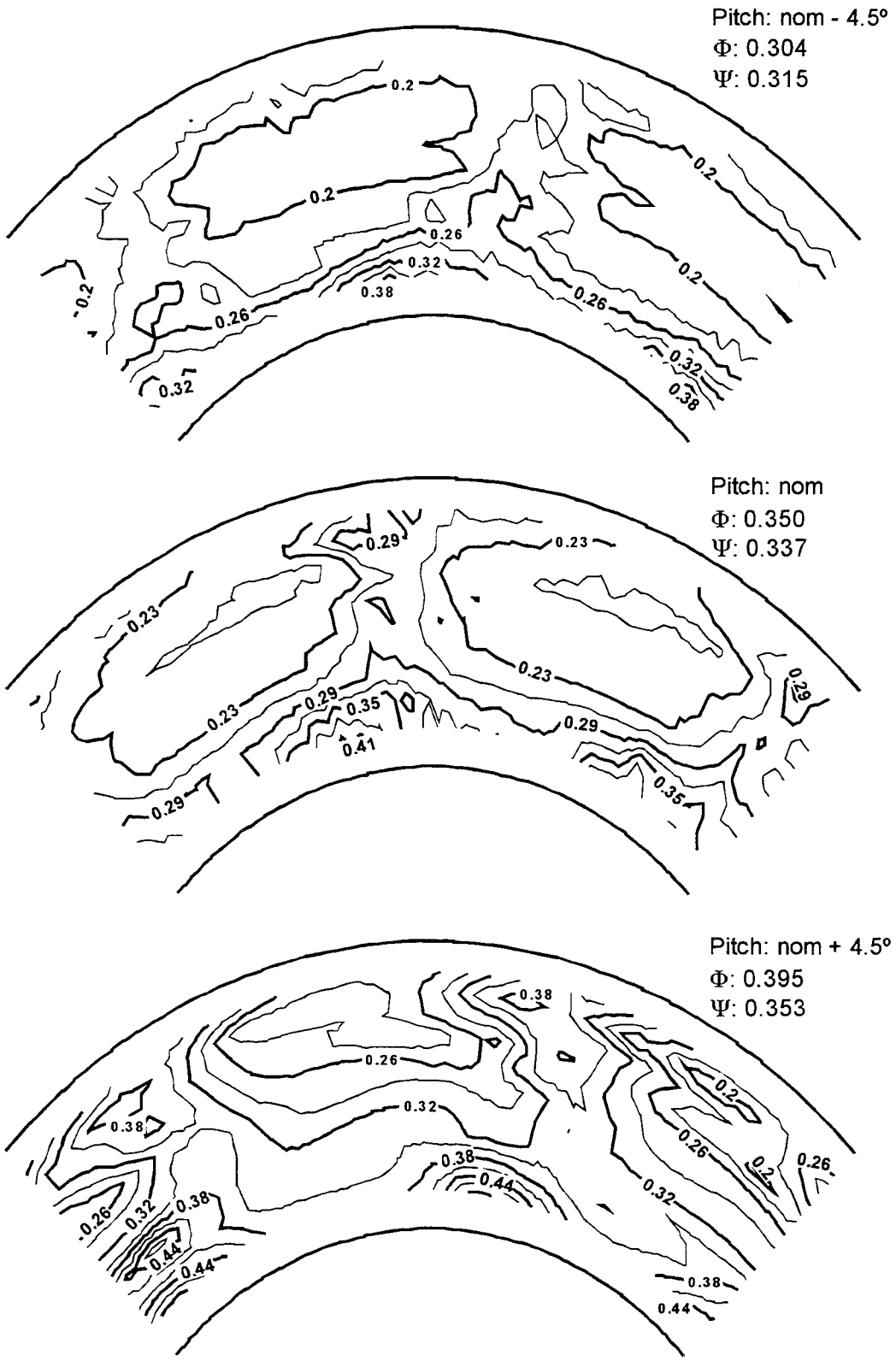

Figure 12. Tangential component map at optimum flow rate for the three pitches tested